



The impact of a mismatch on the interfacial stresses in NanoComposite

Waleed K. Ahmed^{1*}, Sa'ed A. Shakir²

¹ERU, Faculty of Engineering, United Arab Emirates University, Al Ain, UAE.

²Materials Engineering Department, College of Engineering, Al-Mustansireya University, Baghdad, IRAQ.

Received 25 December 2012; Revised 16 March 2013; Accepted 22 March 2013

Abstract

The study investigates the influence of the mismatch on the interfacial stresses in a nanofiber reinforced composite using finite element analysis (FEA). It is assumed that the mismatch exists between the nanofiber and the matrix of the nanocomposite as a defected spot. A representative volume element (RVE) is chosen to model the nanoreinforced composite. The reinforcement properties of the nanofiber are considered as an isotropic for simplification, since the location and the anticipated failure due to mismatch effect is assumed to be along the nanofiber/matrix interface. Therefore, the impact of the transverse properties of the nanofiber is considered as insignificant. Because of complexity of the problem, 2D finite element analysis is carried out to model the nanofiber composite. ANSYS/Mechanical is used to estimate the stresses of the matrix/nanofiber interface. Even though the expected distances between mismatches in the physical phenomenon is random, the investigation proposes to be systematic mismatch. As a consequence, mainly two cases are investigated regarding the mismatch's location. In case one, the mismatch is located along the transverse side of the nanofiber, whereas is positioned in the longitudinal side in the second case. The level of the local interfacial normal and shear stresses arise at the mismatched spot are analyzed using FEA under axial tension. As a result, it is observed that the interfacial stresses increase as the defected area approaches the nanofiber end.

Keywords: FE; interfacial; mismatch; nanocomposite; nanofiber.

PACS: 81.05.uj; 02.70.Dh; 78.67.Sc.

1. Introduction

The nanocomposites is one of the fastest growing areas of nanotechnology, since carbon nanotubes have impressive mechanical properties and is intensively used as reinforcements in polymers and other matrices to form what is nowadays is called "Nanocomposite materials" [1-5]. Nanocomposites are a novel class of composite materials where one of the constituents has dimensions in the range 20-200 nm [6]. They can be produced by embedding reinforcement in the form of nanofibres or nanotubes in a matrix such as a polymer in a similar manner to conventional composite materials [7]. In the recent

*) For correspondence, Tel: + (971) 3 7135328, Fax: + (971) 3 7134975, E-mail: w.ahmed@uaeu.ac.ae

years, the nano applications has introduced in the whole life sectors, starting from nanodevices for electrical [8] and organic applications [9] as well as nanofluid [10], whereas nanomaterials nowadays are utilized in the renewable and green energy sectors [11].

In particular, nanocomposite is fascinating for the fact that it is a bottom-up process, unlike the traditional method of producing engineering components from raw materials [12]. Industries, even aerospace has already benefited from the introduction of conventional composite materials with high strength reinforcements such as carbon fibers. The use of nanotubes which can be 50-100 times stronger than steel and six times lighter, making nanocomposites a key candidate for aerospace applications [13]. Besides, it was shown that nanotubes increase composite strength by as much as 25% [14, 15]. Reinforcement materials for nanocomposites may include nanofibers, nanoplatelets and nanoclay. These reinforcements are functionalized with additives, by this means resulting in a strong interfacial bond with the matrix [6].

In general, the main three mechanisms of interfacial load transfer are the weak van der Waals force between the matrix and the reinforcement, chemical bonding and micromechanical interlocking [16]. Mainly, there are two causes behind a mechanically strong or weak nanocomposite material, the matrix interface with the nanofibres and the stress transfer. Therefore, efforts are done to make this interaction strong [12]. As the nanocomposite subjected to mechanical loading, stress concentrations will take place at the matrix/nanofibre interface which will eventually lead to damage nucleation, initiation, growth and final nontolerated failure [12]. There are two probable sources of damage nucleation in nanocomposites, poor wetting of the nanofibres by the polymer and the aggregation of the nanofibres [17]. Both cases produce polymer rich nanocomposite portions that are likely to experience low stress to failure. Researchers [18] have observed that one of the reasons that nanocomposites may have a low strain to failure is the high interfacial stress that can lead to nanofibre/matrix debonding. In addition, the stress transfer from the matrix to the reinforcement is the main factor that will dictate the final nanocomposite material strength. It is reported that load transfer through a shear stress mechanism was observed at the molecular level [6]. So far, it has been difficult to quantify the improved interfacial bonding between the matrix and the nanofibers accurately, either by direct measurement at the nanoscale [6]. Up to now, it has been quite complicated to evaluate the improved interfacial bonding between the matrix and the nanofibers accurately at the nanoscale level by direct measurement techniques, but it is quite easy to estimate the mechanical properties of the final macroscale nanocomposite materials with different types of standard tests for engineering materials [6]. A uniform dispersion and good wetting of the nanofibers within the matrix must be guaranteed in order to get the maximum utilization of the properties of nanofibers [6]. Moreover, local interfacial properties affect the macrolevel material behavior, like reduction in flexural strength in nanotube/epoxy composite beams due to weakly bonded interfaces [19], as well the reduction in composite stiffness which was attributed to local nanofibers waviness [20, 21]. It was reported that local interfacial stress level in nanocomposites would be much higher than that in traditional composites because of high property mismatch between the nanoscale reinforcement and the matrix. Since high interfacial stress may lead to interfacial debonding and then final failure of nanocomposites, this may contribute to the low failure strains in nanocomposites seen in many experiments [22], whereas the impact of the nanoholes existence on the interfacial stresses in nanocompaosite was investigated using finite element method [23]. Moreover, finite element analysis in particular was used to study the influence of the flexural loading [24] and the nanoinclusion [25] on failure of the nanocomposite. In general, the benefit of small diameters of nanotubes is an increased interfacial contact area with the matrix, while its shortcoming is a high possibility of initial interfacial defects, which may lead to low failure

strain of nanocomposites [6]. Consequently, a theoretical analysis of interfacial stress transfer mismatch between the nanoscale reinforcement and the matrix will be highly required before designing and producing nanocomposite materials [6, 12].

In this context, the present paper discuss through using the finite element technique the consequences of an interfacial defect, i.e., mismatch, which is located between the nanofiber and the matrix of a nanocomposite on the behavior of the nanocomposite. Therefore, the impact of the mismatch is studied and discussed. Uniaxial load is proposed in the study through two cases. The first case when the mismatch located along the transverse side of the nanofiber in order to study the interfacial stresses on both transverse and the longitudinal sides of the nanofiber. Similarly in the second case when the mismatch is positioned in the longitudinal side of the nanofiber to investigate the interfacial stresses at the both sides of the nanofiber. Each case are investigated individually through using traditional software ANSYS/Mechanical to predict interfacial stresses at the interface between the matrix and the nanofiber. Representative volume element (RVE) is proposed to model the case, and two dimensional analyses are implemented to model the nanocomposite because of the complexity of the problem.

2. Finite Element Modeling

Many studies and researches have used the finite element analysis (FEA) as the primary tool to investigate the interfacial stresses and the failure strains of the nanocomposites instead of molecular dynamic simulation [6]. Since the latter can only deal with physical phenomena at the level of a few nanometers at the present stage, the size of a representative volume of a nanocomposite material ranges from 10nm upward to several hundreds of nanometers.

It was reported that mostly the smallest dimension of the nanofiber under investigation of the researchers lies in the range 20-50nm [6], therefore continuum mechanics assumptions, like the one used in the finite element analysis are still valid at such length scales. Analogous finite element analyses have been reported by Fisher et al. [20] with a focus on stiffness analysis incorporating micromechanics theory. In fact, these finite element analyses simplified the complex interaction among the nanoscale reinforcement, matrix and the doable interphase [6].

Although the applicability of continuum mechanics (including micro mechanics) to nanocomposites has been subjected to debate [21, 26], many works directly applying continuum mechanics to nanostructures and nanomaterials have reported meaningful results and elucidated many issues [27-36].

In this paper, the aim of the finite element analysis (FEA) is to investigate the impact of a proposed mismatch between the matrix and the reinforcement, i.e., nanofiber, by estimating the interfacial stresses (σ_x , σ_y , σ_{xy}) along the nanofiber sides. The FEA modeling was carried out using ANSYS/Mechanical software. In order to simplify the modeling of the study, two dimension analyses were conducted by FEA which is mainly based on the representative volume element (RVE) of the nanocomposite material, since the present analysis based on investigating the impact of the mismatch on the failure of the nanocomposite, where the orientation of the mismatch is proposed to be along the longitudinal direction only of the nanofiber/matrix interface, therefore the other direction of failure is eliminated. Besides, constituents properties of the nano-reinforcement and the matrix have been obtained used similar to the previous investigators [6]. The model and the boundary condition used in this study is shown in Figure 1a, whereas Fig. 1(b) illustrates the coordinate details around the nanaofiber.

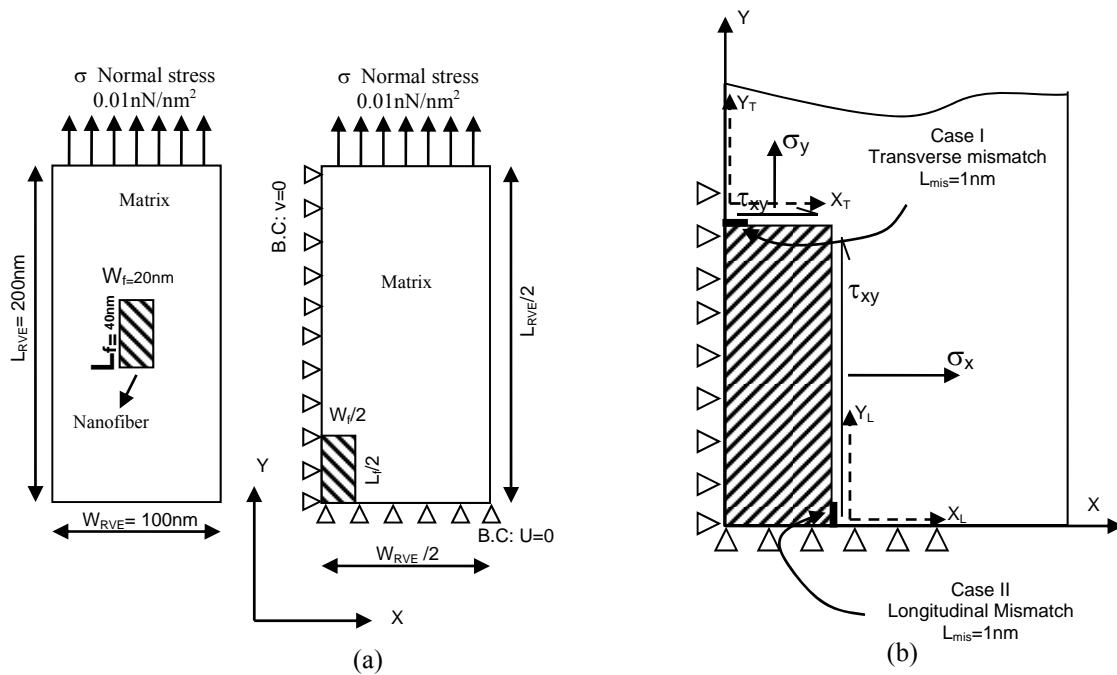


Fig. 1 (a): RVE of the nanocomposite, (b) detailed nanofiber and local coordinate system.

Due to complexity of the problem, 2D finite element analysis is carried out to model the nanofiber composite, i.e., RVE. Eight-node quadrilateral element is employed in the investigation through ANSYS/Mechanical software to assess the interfacial stresses. The interfacial defect, (i.e., the mismatch) is modeled as a debonded spot. Tie constraints are applied locally at the interface between the nanofiber and the matrix except for the mismatched spot in order to represent the defected zone. A dense mesh in and around the nanofiber-matrix interface to a relatively coarser mesh utilized for the rest of the RVE.

3. Materials Specification

The material properties used in the baseline RVE is epoxy matrix has a Young's modulus of $E_m = 2.6$ GPa and Poisson's ratio of $\nu_m = 0.3$, whereas the nanofiber is considered as transversely isotropic materials [18,20] which is similar to other finite element analyses done previously [6]. Since the proposed mismatches through the study are assumed to be located along the nanofiber/matrix interface, the prospective failure will be along the interface and only the longitudinal properties of the nanofiber play the major role in the failure mechanism. The transvers properties has insignificant impact accordingly. The nanofiber is considered as a carbon fiber of elastic modulus of $E_f = 200$ GPa. A tensile stress of 0.01 nN/nm^2 is applied on the nanocomposite and directed parallel to the longitudinal side of the nanocomposite meanwhile the transvers direction of the nanocomposite is not subjected to any load.

The adopted RVE of the proposed nanocomposite is proposed to have a length of $L_{RVE} = 200$ nm and width of $W_{RVE} = 100$ nm [6]. The RVE consist of a matrix of polymer and a nanofiber. The nanofiber has a rectangular shape of $L_f = 40$ nm and $W_f = 20$ nm which is equivalent to $L_f/L_{RVE} = 0.2$ and $W_f/W_{RVE} = 0.2$ which can be expressed by a fiber volume fraction of the nanocomposite $V_f = 4\%$.

The mismatch length of 1nm is considered in the analysis of the two cases, and this value is corresponded to mismatch length to the nanofiber length of $L_{\text{mis}}/L_f = 0.025$, as $L_{\text{mis}}/W_f = 0.05$ with respect to the nanofiber's width. The nanofiber and the matrix in the model are assumed to be bonded perfectly with the exception of the mismatch's faces. Frictionless sliding behavior is assumed between the mismatch's faces.

The level of the local interfacial stresses arises at the mismatched spot are inspected as well. The defected nanocomposite, i.e., mismatched, is investigated under static loading conditions for uniaxial tensile stress. In addition, the defected location along the transverse and the longitudinal side of the nanofiber is considered as parameters in the analysis through the two cases investigated.

In the first case, the impact of the mismatch on the transverse side of the nanofiber is studied for both interfacial normal stresses σ_y and shear stresses σ_{xy} . Mainly three locations of the mismatch are chosen along the nanofiber of $X_T/W_f = 0.05, 0.25$ and 0.5 , where X_T is distance measured from the y-axis to the end of the mismatch along the transverse side of the nanofiber. Besides, the influence of the transverse mismatch is investigated as well on the longitudinal side through estimating the normal stresses σ_x and the shear stresses σ_{xy} .

Conversely, the second case investigates the effect of a mismatch on the longitudinal side of the nanofiber and is studied for three locations which is analogues to $Y_L/L_f = 0.025, 0.25$ and 0.5 , where Y_L is the distance measured from the x-axis to the end of the mismatch along the longitudinal side of the nanofiber. Moreover, the influence of longitudinal mismatch on the interfacial normal stresses σ_y and shear σ_{xy} on the transverse side of the nanofiber is investigated as well.

4. Results and Discussion

In the FE analysis of the RVE which contains either transverse or longitudinal mismatched spot, the impact of the location of the mismatch along the fiber's sides, i.e., the transverse and the longitudinal side on the interfacial normal and shear stresses are investigated.

In case I, the mismatch is presumed to have a length of 1 nm and the location of the mismatch is proposed to be positioned at three locations along the short side. The following general conclusions which can be drawn from the results:

a) The mismatch affects the level of the interfacial stresses on the same side. It is clear that considerable increasing in the normal stresses σ_y stresses of 2.23 to 3.4 times the stresses of the non-mismatch case as the mismatch comes to be at the right tip of the fiber as illustrated in Fig. 2. While the shear stresses σ_{xy} along the same side, i.e., short side, shows an increasing of its value up to 2.4 times the value of the non-mismatch case as shown in Fig. 3, whereas an exceptional reduction of 60% in σ_{xy} arisen in the first location of the mismatch (i.e., $X_T/W_T = 0.05$).

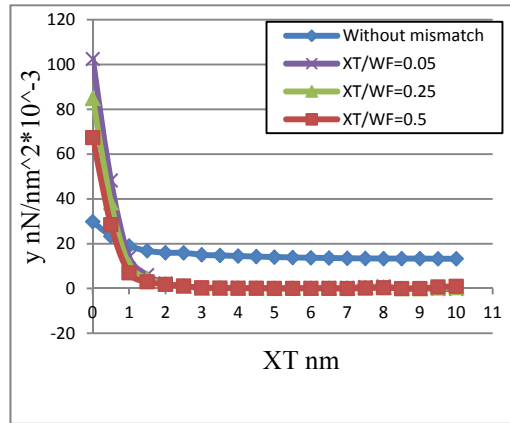


Fig. 2: Interfacial stress distribution (σ_y) along the transverse side of the nanofiber due to transverse

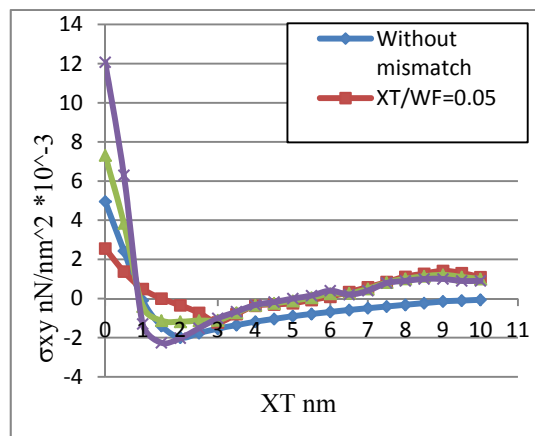


Fig. 3: Interfacial stress distribution (σ_{xy}) along the transverse side of the fiber due to transverse mismatch.

b) In the other hand, the influence of the transvers mismatch on the longitudinal interfacial stresses are investigated. A considerable more consequence on the interfacial stresses on the longitudinal side of the nanofiber can be shown in Fig. 4, where the normal stresses σ_x decreased 3.8 times in in comparison with the non-mismatch case, while the interfacial shear stresses σ_{xy} shows rising in stresses up to 2.5 times with respect to the non-mismatch case as clarified in Figure 5, except when $X_T/W_T = 0.05$, where the decrease in the stresses was 48%.

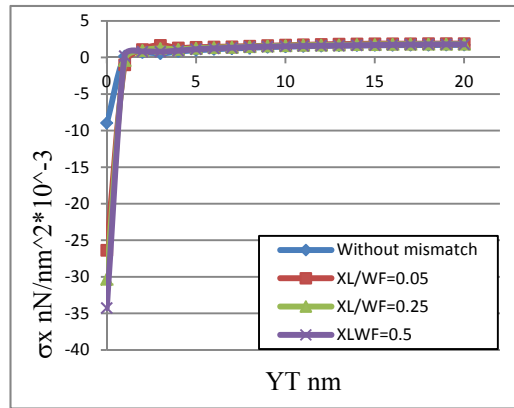


Fig. 4: Interfacial stress distribution (σ_x) along the longitudinal side of the fiber due to transverse mismatch.

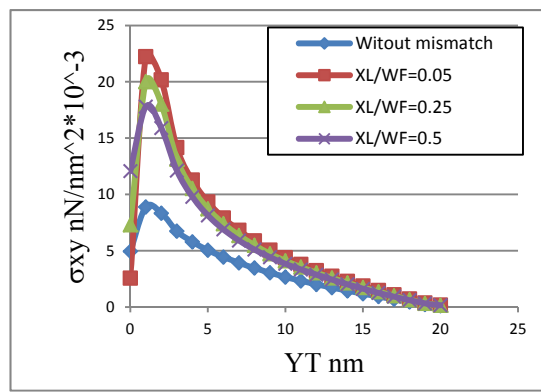


Fig. 5: Interfacial stress distribution (σ_{xy}) along the longitudinal side of the fiber due to transverse mismatch.

In the second case, the following conclusions which can be obtained from the results obtained when the mismatch falls along the longitudinal side of the nanofiber:

- a) It is clear that the normal stress σ_x changes its status from negative to positive value as the mismatch approaches the top edge of the nanofiber, i.e., $Y_L/L_F = 0.05$ as shown in Fig. 6, while the interfacial shear stress σ_{xy} exhibits an increasing of 1.34 times in comparison with the non-mismatched case as the mismatch gets near the top edge of the fiber as illustrated in Fig. 7.

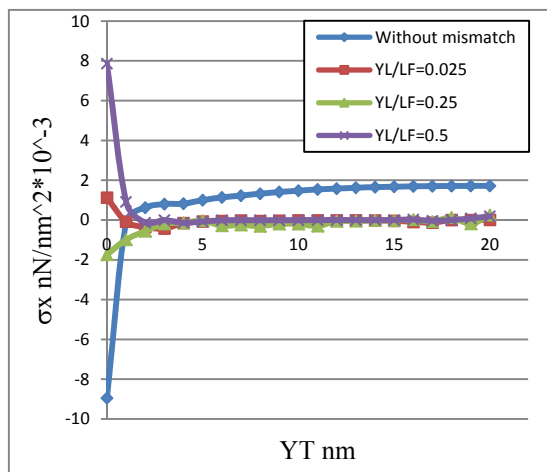


Fig. 6: Interfacial stress distribution (σ_x) along the longitudinal side of the fiber.

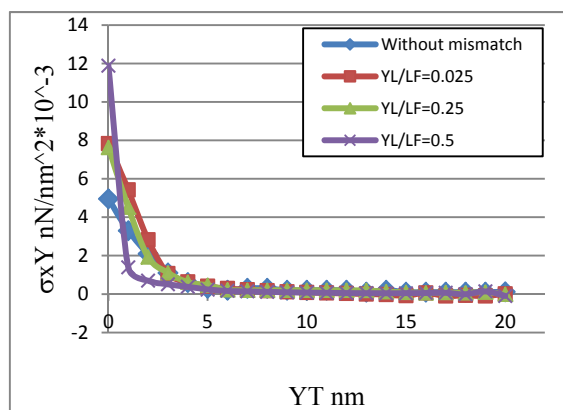


Fig. 7: Interfacial stress distribution (σ_{xy}) along the longitudinal side of the fiber.

b) The last investigation is done to estimate the transverse interfacial stresses σ_y and σ_{xy} due to the change in the longitudinal mismatch's location. The effect of existing mismatch in the longitudinal side of the nanofiber shows a considerable increasing of a maximum interfacial normal stress σ_y up to 1.67 on the short side of the fiber as shown in Figure 8 at $Y_L/L_F = 0.025$, while a maximum increase of shear stress σ_{xy} of 2.38 time the no-mismatch case along the transverse side as shown in Fig. 9.

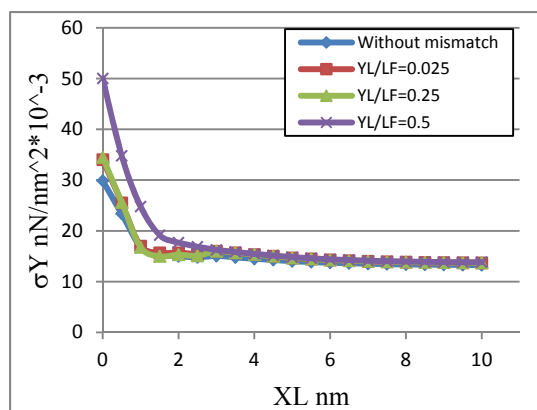


Fig. 8: Interfacial stress distribution (σ_y) along the transverse side of the fiber.

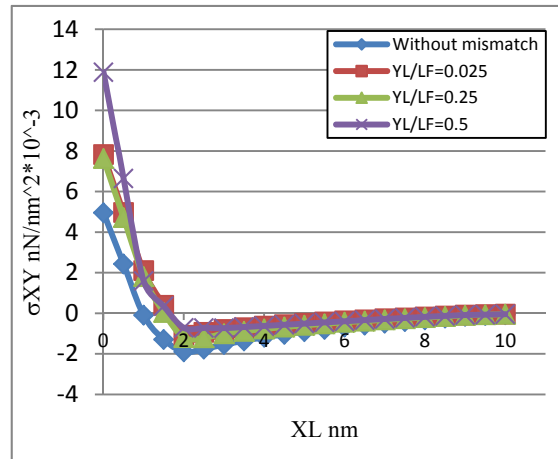


Fig. 9: Interfacial stress distribution (σ_{xy}) along the transverse side of the fiber.

5. Conclusion

In this numerical investigation it has been proved that of mismatch existence around a nanofiber in a RVE of nanocomposite has a great influence on the increasing of the interfacial stresses between the nanofiber and the matrix. The location of the mismatch toward the tip of the nanofiber increases the interfacial stresses many time compared with the non-mismatch case for both transverse and longitudinal location of the mismatch, while the middle location of the mismatch has the lowest influence on the increasing the interfacial stresses.

References

- [1] M. M. J. Treacy, T. W. Ebbesen, T. M. Gibson, *Nature* **381** (1996) 678
- [2] K. T. Lau, D. Hui, *Comp.* **B33** (2002) 263
- [3] D. Qian, G. J. Wagner, W. K. Liu, Y. Min-Feng, R. S. Ruof, *Appl. Mech. Rev.* **55** (2002) 495
- [4] J. J. Luo, I. M. Daniel, *Comp. Sci. Technol.* **63** (2003) 1607
- [5] H. D. Wagner, O. Lourie, Y. Feldman, R. Tenne, *Appl. Phys. Lett.* **72** (1998) 188
- [6] L. Roy Xu, S. Sengupta, *J. of Nanoscience and Nanotech.* **10** (2005) 1-6
- [7] P. M. Ajayan, L. S. Schadler, P. V. Braun, *Nanocomposite Science and Technology*, Wiley-VCH Verlag GmbH Co. K GaA, Weinheim **77** (2003)
- [8] A. Chaudhry, J. N. Roy, *Int. J. Nanoelectronics and Materials* **5** (2012) 1-9
- [9] P. A. Priya, C. P. Kala, D. J. Thiruvadigal, *Int. J. Nanoelectronics and Materials* **3** (2010) 1-7
- [10] I. S. Mohamad, S. T. Chitrambalam, S. B. A. Hamid, *Int. J. Nanoelectronics and Materials* **5** (2012) 25-30
- [11] M. Bououdina, *Int. J. Nanoelectronics and Materials* **3** (2010) 155-167
- [12] M. Bourchak, B. Kada, M. Alharbi, K. Aljuhany, *Int. J. of Nanoparticles* **2** (2009) 467-475
- [13] J. Njuguna, K. Pielichowski, *Adv. Eng. Mat.* **6** (4) (2004) 204-210

- [14] D. Qian, E. C. Dickey, R. Andrews, T. Rantell, *Appl. Phys. Lett.* **76** (2000) 2868
- [15] M. F. Yu, O. Lourie, M. Dyer, Moloni K, T. Kelly, R. S. Ruoff, *Science* **287** (2000) 637
- [16] L. S. Schadler, S. C. Giannaris, P. M. Ajayan, *Appl. Phys. Lett.* **73** (1998) 3842
- [17] L. R. Xu, V. Bhamidipati, W. Zhong, J. Li, C. M. Lukehart, E. Lara Curzio, K. C. Liu, M.J. Lance, *J. Comp. Mat.* **38** (18) (2004) 1563-1582
- [18] L. R. Xu, S., *J. Nanosci. Nanotech.* **5** (4) (2005) 620-626
- [19] K. T. Lau, S. Q. Shi, L. M. Zhou, H. M. Cheng, *J. Comp. Mater.* **37** (2003) 365
- [20] F. T. Fisher, R. D. Bradshaw, L. C. Brinson, *Comp. Sci. Technol.* **63** (2003) 1689
- [21] D. Srivastava, C. Wei, K. Cho, *ASME Appl. Mech. Rev.* **56** (2003) 215
- [22] L. R. Xu, V. Bhamidipati, W. H. Zhong, J. Li, C. M. Lukehart, E. Lara-Curzio, K. C. Liu, Lance M. J, *J. Comp. Mater.* **38** (2004) 1563
- [23] W. K. Ahmed, S. A. Shakir, *Proceedings of the International Conference on Bio-Nanotechnology: Future Prospects in the Emirates*, Al Ain, UAE, pp.241-245, November 18-21 (2006). ISBN 9948-02-135-5
- [24] Waleed K. Ahmed, Wail N. Al Rifaie, Yarub Al-Douri, *Proceedings of the 2nd Saudi International Nanotechnology Conference 2012 (2SINC)*, KACST, Riyadh, Saudi Arabia, pp.85, November 11-13, (2012)
- [25] W. Kh. Ahmed, F. Kh. Omar, Y. Haik, *First Sharjah International Conference on Nanotechnology and Its Applications*, Sharjah, UAE, pp.111, April 10-12, (2007): American Institute of Physics. DOI:10.1063/1.2776685, Bibliographic Code:2007AIPC.929.38A
- [26] FT. Fisher, LC. Brinson, *Handbook of theoretical and computational nanoscience*, American Scientific Publishers (2006)
- [27] D. Srivastava , CY. Wei, K. Cho, *Appl. Mech Rev.* **56** (2003) 215-30
- [28] MJ. Leamy, *Int. J. Solids Struct.* **44** (2007) 874-94
- [29] GM. Odegard, TS.Gates, *J. Intell. Mater. Syst. Struct.* **17** (2006) 239-46
- [30] A. Sears, RC. Batra, *Phys. Rev.* **B73** (2006) 085410-1-085410-11
- [31] M. Arroyo, T. Belytschko, *Meccanica* **40** (2005) 455-469
- [32] GM. Odegard, TC. Clancy, TS. Gates, *Polymer* **46** (2005) 553-62
- [33] M. Arroyo, T. Belytschko, *Int. J. Numer. Methods Eng.* **59** (3) (2004) 419-56
- [34] LJ. Zhu, KA. Narh, *J. Polym. Sci.* **42** (2004) 2391-406
- [35] YP. Wu, QX. Jia, DS. Yu, LQ. Zhang, *Polym. Testing* **23** (2004) 903-909
- [36] TD. Fornes, DR. Paul, *Polymer* **44** (2003) 4993-5013